Floquet stability analysis of the wake of an inclined flat plate

Dan Yang, Bjørnar Pettersen, Helge I. Andersson, and Vagesh D. Narasimhamurthy

Citation: Physics of Fluids (1994-present) **25**, 094103 (2013); doi: 10.1063/1.4820815
View online: http://dx.doi.org/10.1063/1.4820815
View Table of Contents: http://scitation.aip.org/content/aip/journal/pof2/25/9?ver=pdfcov
Published by the AIP Publishing

PHYSICS OF FLUIDS **25**, 094103 (2013)

Floquet stability analysis of the wake of an inclined flat plate

Dan Yang,[1,a)] Bjørnar Pettersen,[1] Helge I. Andersson,[2] and Vagesh D. Narasimhamurthy[2]
[1]*Department of Marine Technology, Norwegian University of Science and Technology, Trondheim NO-7491, Norway*
[2]*Department of Energy and Process Engineering, Norwegian University of Science and Technology, Trondheim NO-7491, Norway*

(Received 13 December 2012; accepted 13 August 2013; published online 18 September 2013)

The route from a time-periodic two-dimensional wake flow to a three-dimensional flow has been investigated by means of linear Floquet stability analysis. The critical Reynolds number for the onset of three-dimensional instabilities in the wake behind a flat plate with an angle of attack α in the range from 20° to 30° with respect to the free stream was determined. For all three angles considered, in the lower wavelength range, the two-dimensional base flow first became unstable with respect to the sub-harmonic mode C. Although the critical Reynolds number decreased with increasing angle of attack, the spanwise wavelength remained close to two times the projected plate width. Qualitatively different transition scenarios were obtained for the three angles of attack with a particularly simple scenario for $\alpha = 30°$. © *2013 AIP Publishing LLC*. [http://dx.doi.org/10.1063/1.4820815]

I. INTRODUCTION

The flow around bluff bodies has been studied extensively due to its practical importance of both engineering and theoretical relevance in fluid dynamics. The transition from two- to three-dimensional flow in the wake is a substantial topic to understand. The flow experiences significant changes during the transition process. In his experimental studies, Roshko[1] first observed the existence of a transition regime in the wake of bluff bodies and reported distinct irregularities in the wake velocity fluctuation.

During the previous decades, much attention has been paid to flow past circular and square cylinders because their geometrical simplicity allowing researchers to perform intensive numerical and experimental investigations. The experimental investigation of Williamson[2] was the first to demonstrate the existence of two stages in the transition to three-dimensionality of a cylinder wake. These two stages were identified as mode A and mode B with dominant spanwise wavelength of approximately three to four diameters and one diameter (Williamson[3]) for the two modes, respectively. The experimental observations were confirmed by the numerical linear Floquet stability analysis of Barkley and Henderson.[4]

The critical Reynolds numbers for mode A (Re_A) and mode B (Re_B) have been consistently reported even with different investigation methods. The study of Williamson[3] revealed $Re_A \approx 190$ and $Re_B \approx 230 - 260$. Barkley and Henderson[4] reported $Re_A \approx 188$ and $Re_B \approx 259$. Posdziech and Grundmann[5] found $Re_A \approx 190.2$ and $Re_B \approx 261$.

Robichaux *et al.*[6] performed a Floquet stability analysis of the wake of a square cylinder. The dominant three-dimensional instabilities are similar to those for the circular cylinder with the critical Reynolds number of $Re_A \approx 166$ and $Re_B \approx 190$. The corresponding spanwise wavelengths are 5.22 and 1.2 times the square cylinder height. A further instability mode which has a wavelength between

a)dan.yang@ntnu.no

mode A and mode B occurred at a higher critical Reynolds number of 200 and was labeled as mode S by Robichaux *et al.*[6] The study of Blackburn and Lopez[7] subsequently showed that this mode was not a subharmonic mode, but was a mode with complex Floquet multipliers.

A new type of instability (called mode C) was found in the wake of a bluff ring, i.e., essentially a curved circular cylinder (Sheard *et al.*[8]). Carmo *et al.*[9] also found a mode C instability in the flow past two staggered circular cylinders. It was reported that mode C is promoted in asymmetric flow configurations with a period twice that of the vortex shedding period. The mode C instability was also found in the flow past an inclined square cylinder (Fitzgerald *et al.*,[10] Sheard *et al.*,[11] Sheard,[12] and Yoon *et al.*[13]). The above-mentioned studies detected mode C by means of a Floquet stability analysis. However, in an earlier experimental study Zhang *et al.*[14] surprisingly observed a mode C by placing a control wire parallel to the axis of a circular cylinder.

In the study of Blackburn and Sheard,[15] the relationship between quasi-periodic and subharmonic instability modes and how it is influenced by wake symmetry breaking was investigated. In their square cylinder wake study, the symmetry is broken by a small fixed rotation of the cylinder about its axis.

Linear Floquet stability analysis is a common technique to calculate the stability of a flow exposed to three-dimensional perturbations. When the disturbance is small, the growth of the instability is linear, and then the nonlinear terms in the system can be neglected. However, the linear growth cannot be sustained forever. When the growth becomes nonlinear, we have to depend on experiments or three-dimensional numerical simulations. In Floquet stability analysis, we superimpose an infinitely small three-dimensional perturbation onto the two-dimensional base-flow, and measure the temporal development of the perturbation. Description of this method is found in Barkley and Henderson.[4] Although secondary instabilities arise naturally in flow simulations when the full, i.e., nonlinear and three-dimensional, Navier-Stokes equations are solved, a Floquet stability analysis represents a simplified approach to identify the critical Reynolds number at which a three-dimensional instability occurs, together with its wavelength. Successful applications of this method in different wake flows are found in Blackburn *et al.*,[16] Ryan *et al.*,[17] Kevlahan,[18] Carmo *et al.*,[9,19] Gioria *et al.*,[20] Nazarinia *et al.*,[21] Jacono *et al.*,[22] Richter *et al.*,[23] and Choi *et al.*[24]

The flow past a flat plate oriented perpendicular to the free stream, i.e., with 90° angle of attack, separates from the sharp edges of the plate. In the short review of Thompson *et al.*,[25] the transition process in the wake of a flat plate normal to the free stream involves two unstable modes. First, the long wavelength mode becomes unstable at Reynolds number of 105–110, with a wavelength of approximately $5 - 6d$, where d is the height of the plate. Second, the shorter wavelength mode becomes unstable at Reynolds number of approximately 125, with a wavelength of $2d$.

Meneghini *et al.*[26] numerically investigated the flow around a stalled NACA0012 airfoil at angle of attack 20°. A subharmonic (mode C) and a quasi-periodic mode were found with wavelengths of approximately $0.57c$ and $2.1c$ (c is the chord length of the airfoil), respectively. The critical Reynolds numbers based on c were around 456 and 580 for the two modes.

In the present study, we performed a Floquet stability analysis on flow past an inclined flat plate on the secondary instability leading to three-dimensional flow. The angle of attack range is chosen to be $20° - 30°$, in which it has been shown that the flow experiences a complex transition process to chaos (Zhang *et al.*[27]). In addition, the present authors have recently reported complex transition phenomena in the wake of an inclined flat plate using direct numerical simulation (DNS) for attack angles 20° and 25° (Yang *et al.*[29,32]). Nevertheless, performing DNS in a parametric study covering a wide range of Reynolds numbers and attack angles is a computationally demanding task. We have therefore identified Floquet stability analysis as the right tool to further explore the transition phenomena with detailed insights into the critical Reynolds number and instability mode wavelengths in the present problem.

II. METHODOLOGY

In the present study, the base flows were obtained by means of two-dimensional numerical simulation of the incompressible Navier-Stokes equations, written in non-dimensional form as

$$\frac{\partial \boldsymbol{u}}{\partial t} + (\boldsymbol{u} \cdot \nabla)\,\boldsymbol{u} = -\nabla p + \frac{1}{Re}\nabla^2 \boldsymbol{u}, \tag{1}$$

$$\nabla \cdot \boldsymbol{u} = 0. \tag{2}$$

The Reynolds number is defined as $\mathrm{Re} = U_0 d / \nu$, where U_0 is the free-stream velocity and d is the plate width. A spectral-element method is used to solve the time-dependent equations. Details of the computational solver (VIPER) can be found in Sheard *et al.*[30] and Sheard and Ryan.[31] To generate the base flow, Eqs. (1) and (2) are solved in two dimensions.

Based on the Floquet theory, the stability analysis is performed by decomposing the velocity and pressure field $(\boldsymbol{u}, p)$ into a two-dimensional base flow $(\boldsymbol{U}, P)$ and a three-dimensional disturbance $(\boldsymbol{u}', p')$,

$$\boldsymbol{u} = \boldsymbol{U} + \boldsymbol{u}', \tag{3}$$

$$p = P + p'. \tag{4}$$

Substituting Eqs. (3) and (4) into Eqs. (1) and (2), cancelling the base flow terms and neglecting products of the perturbation field, yields the linearized Navier-Stokes equations,

$$\frac{\partial \boldsymbol{u}'}{\partial t} + (\boldsymbol{U} \cdot \nabla)\,\boldsymbol{u}' + \left(\boldsymbol{u}' \cdot \nabla\right)\boldsymbol{U} = -\nabla p' + \frac{1}{Re}\nabla^2 \boldsymbol{u}', \tag{5}$$

$$\nabla \cdot \boldsymbol{u}' = 0. \tag{6}$$

Linear stability analysis is then performed to determine the leading eigenmodes of the stability problem. The eigenvalues correspond to Floquet multipliers (μ) and eigenvectors yield the mode shape of the perturbation field. For details, see Sheard *et al.*[11] A Floquet multiplier $|\mu| > 1$ corresponds to a positive growth rate and an unstable mode. For different types of the multipliers, the instability modes can be classified as follows: regular modes (mode A and B) have Floquet multipliers containing only positive real part, subharmonic mode (mode C) has only a negative real part, and quasi-periodic mode (mode QP) arises from a complex-conjugate pair of multipliers with a non-zero imaginary part (Sheard *et al.*[11]).

The two-dimensional mesh used to discretize the Navier-Stokes equations for an inclined flat plate is shown in Fig. 1. The domain size and element distribution were kept constant for the incidence angles investigated, 20°, 25°, and 30°. The computational domain extends $15d$ upstream,

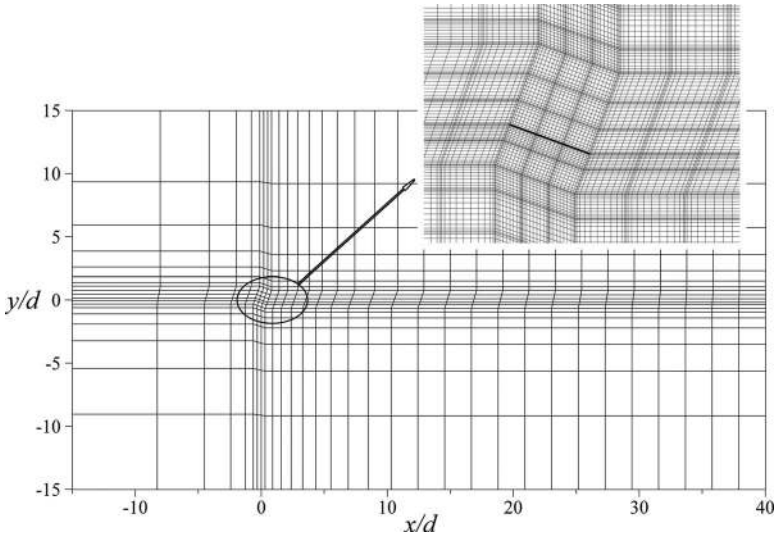

FIG. 1. The complete computational domain and mesh details in the vicinity of the plate at angle of attack 20°. The plate is indicated by a thick line.

TABLE I. Convergence of global quantities with different order N for $Re = 500$ and $\alpha = 20^\circ$. The global quantities: Strouhal number St, mean and fluctuating drag coefficients, C_D and C'_D, and mean and fluctuating lift coefficients, C_L and C'_L. The Floquet multipliers are calculated at $\lambda / d = 0.875$.

N	St	C_D	C_L	C'_D	C'_L	$\lvert\mu\rvert$
6	0.5341	0.4531	0.9917	0.0203	0.0945	...
8	0.5035	0.4440	0.9708	0.0178	0.1023	...
10	0.4959	0.4447	0.9732	0.0173	0.0996	...
12	0.4959	0.4463	0.9786	0.0177	0.1006	1.027
14	0.4959	0.4472	0.9823	0.0176	0.1003	1.007

$40d$ downstream, and $15d$ to each side of the center of the plate. The domain is divided into 589 macroelements. Each element contains N × N interpolation nodes. Free-stream boundary conditions were enforced at the upstream and lateral boundaries, while a Neumann-type boundary condition was employed at the outlet. At the plate surface, a no-slip boundary condition was used.

In order to determine the most efficient mesh resolution for the present simulation, a grid resolution study was performed. The time step adopted in these simulations is $0.002d / U_0$. The results given in Table I with varying number of mesh nodes show small differences of the global quantities for order $N \geq 12$, and $N = 12$ was therefore used for the simulations.

III. RESULTS AND DISCUSSION

In this section, the Floquet multipliers based on the variation of Reynolds number and spanwise wavelength are presented first for the three angles of attack, followed by the mode characteristics analysis. The Reynolds number simulated is less than 600 for all angles of attack.

A. Floquet analysis

The main objective of the linear Floquet stability analysis is to determine the critical values of Reynolds number Re and the corresponding spanwise wavelength λ for which the two-dimensional wake becomes linearly unstable, i.e., in the region when $|\mu| > 1$. Figure 2 shows the results for the angle of attack 20° case. In Fig. 2(a), as Re increases, the multiplier branches have similar tendencies, which are consistent with negative real multipliers at short wavelengths, positive real multipliers as the wavelength is approximately larger than $3.5d$, and complex-conjugate multipliers in the middle of the wavelength range from about d to $3.5d$ shown in Fig. 2(a).

At this angle of attack, the flow first becomes unstable to a longer wavelength mode, shown in Fig. 2(a). At Reynolds number of $Re \approx 400$, the wake also becomes unstable to a second mode, with a spanwise wavelength $\lambda / d \approx 0.7$, see Fig. 2(b). As the Re increases, the absolute value of the maximum multiplier grows and shifts to a slightly higher wavelength, see Fig. 2(b). A number of stable quasi-periodic Floquet multipliers are obtained over a wavelength range $1.0d - 3.5d$.

Figures 2(c) and 2(d) show the results for the simulations at Reynolds numbers 475, 500, and 525. Here, the wakes become unstable to the quasi-periodic mode. Unlike the negative real multipliers in Fig. 2(b), the peak multipliers in Fig. 2(d) decrease and shift to larger wavelengths as the Reynolds number is increased. The instability mode now becomes critical at around $Re \approx 500$ with critical spanwise wavelength of $\lambda / d \approx 0.875$.

As the Reynolds number increases to 550, 575, and 600, in Figs. 2(e) and 2(f), a quasi-periodic mode at wavelength range of $0.5d - 0.7d$ is pronounced with almost constant spanwise wavelength. In this Reynolds number range, an instability mode with negative real multipliers appears again at $1.0 \lesssim \lambda / d \lesssim 1.5$, as found in Figs. 2(a) and 2(c). The peak multipliers increase and shift to larger wavelengths as Re increases, see Fig. 2(f).

The results for the case of angle of attack 25° are presented in Fig. 3. The wake first becomes unstable to a short wavelength mode with negative real multipliers, at the wavelength region $\lambda \lesssim 1.2d$. The critical Reynolds number for this mode is $Re \approx 266$ with a spanwise wavelength of

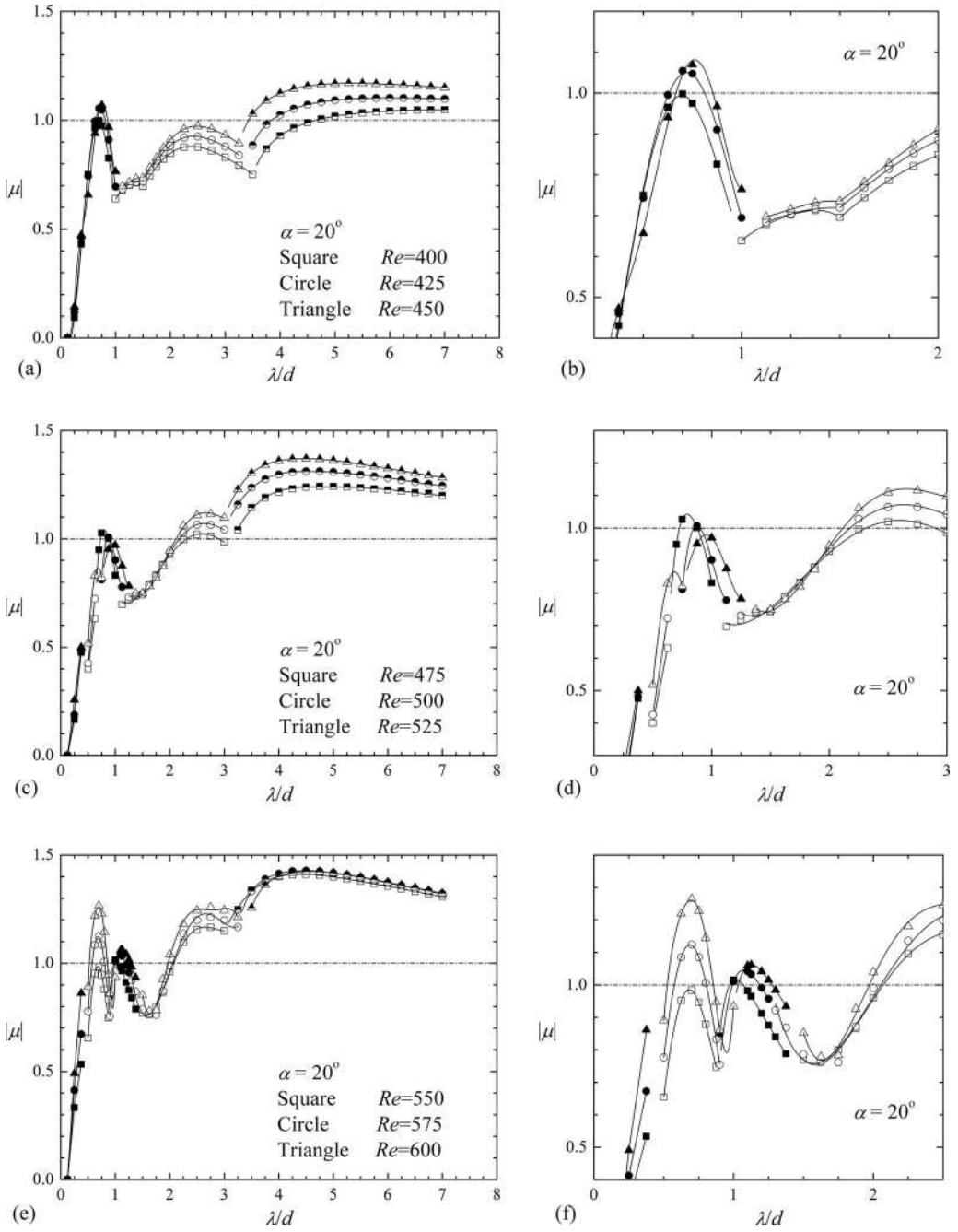

FIG. 2. Moduli of the Floquet multipliers $|\mu|$ versus spanwise wavelength λ for different Reynolds numbers at $\alpha = 20°$. Filled symbols show negative real Floquet multipliers, open symbols correspond to complex-conjugate Floquet multipliers, and half-filled symbols represent positive real Floquet multipliers. Images (b), (d), and (f) show the details corresponding to images (a), (c), and (e), respectively.

$\lambda / d \approx 0.826$, shown in Fig. 3(a). The peak position of the multipliers in this mode keeps constant as *Re* increases. The flow is subsequently unstable to a quasi-periodic mode, as *Re* becomes larger than 280 at the spanwise wavelength of $\lambda / d \approx 2.697$. Figure 3(b) shows the critical Reynolds numbers for this mode (the open symbols).

At angle of attack 25°, a subharmonic frequency was excited in the base flow as $Re > 305$. Therefore, two vortex shedding cycles were used for the Floquet calculation as $Re > 305$. In the simulations of Carmo *et al.*,[9] two vortex shedding periods were used for the Floquet analysis for flow

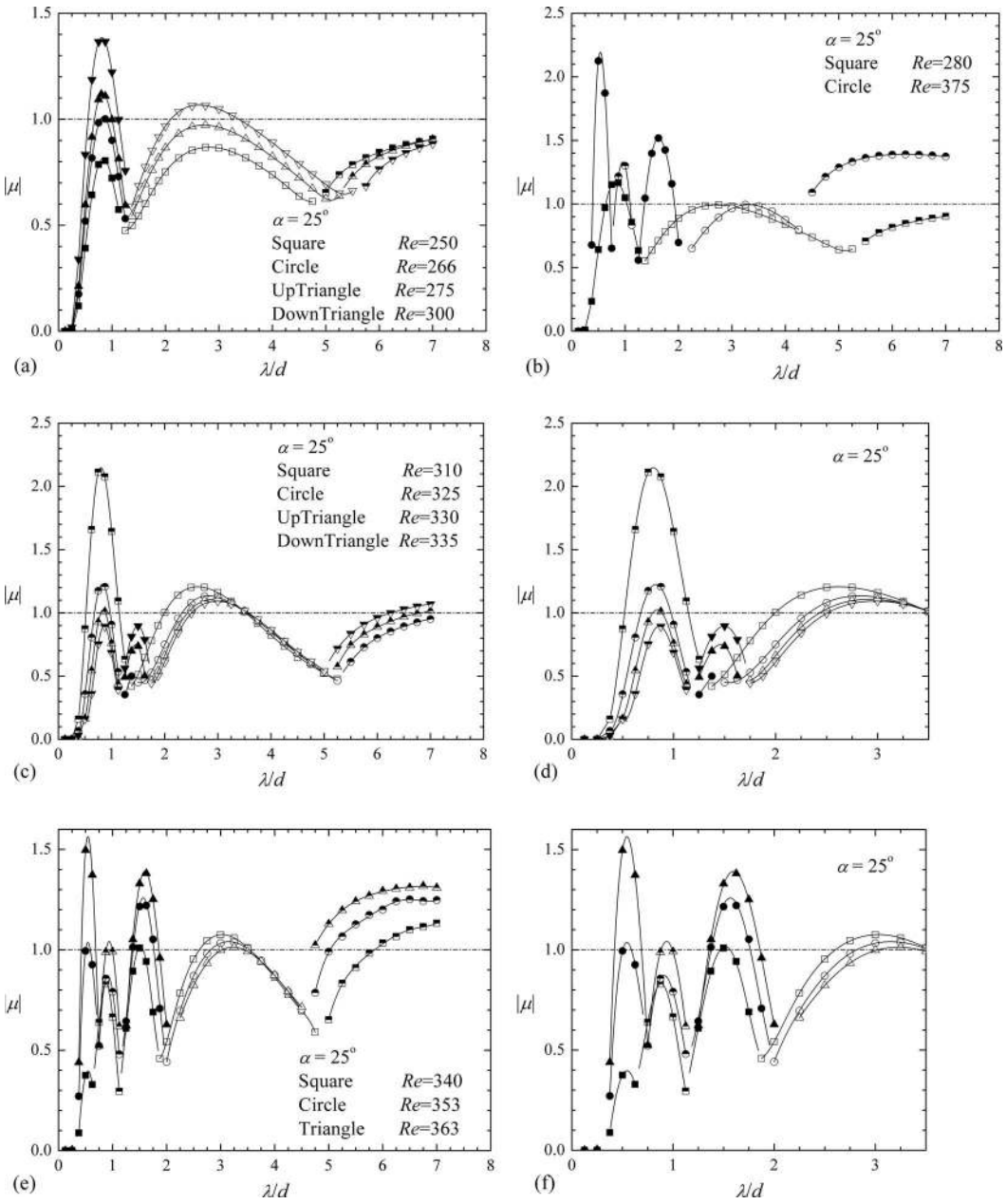

FIG. 3. Moduli of the Floquet multipliers $|\mu|$ versus spanwise wavelength λ for different Reynolds numbers at $\alpha = 25^\circ$. Filled symbols show negative real Floquet multipliers, open symbols correspond to complex-conjugate Floquet multipliers, and half-filled symbols represent positive real Floquet multipliers. Images (d) and (f) show the details corresponding to images (c) and (e), respectively.

past two staggered circular cylinders, since in their simulations the far wake had period twice that of the vortex shedding. The results in Figs. 3(c) and 3(d) show that the flow is unstable to a mode with positive real multipliers. This instability mode is located in the same wavelength region as is shown in Fig. 3(a). The multiplier peaks for the present mode decrease as *Re* increases. Figure 3(c) shows that the multiplier peaks for the quasi-periodic mode are decreased as *Re* increases. Figure 3(c) also reveals that a number of negative real Floquet multipliers appear between the short wavelength mode and the quasi-periodic mode.

As *Re* increases further, as shown in Figs. 3(e) and 3(f), the three different simulations each contains four distinct peaks of Floquet multipliers, corresponding to four synchronous instability

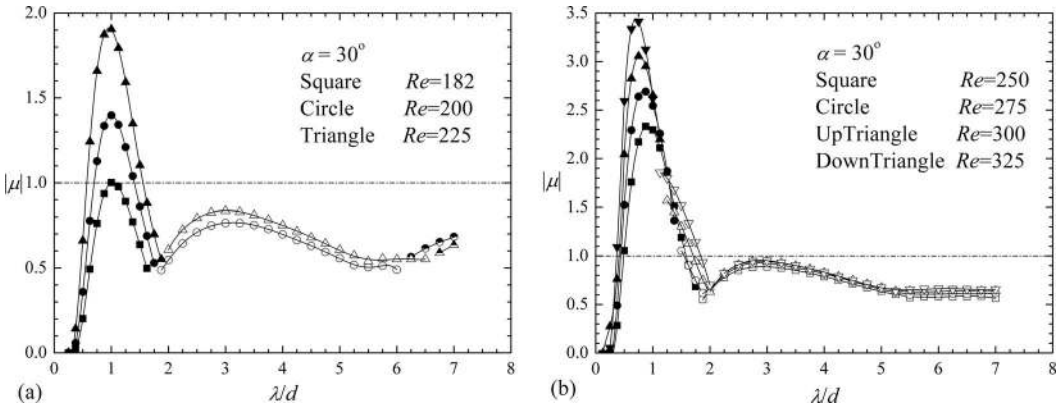

FIG. 4. Moduli of the Floquet multipliers $|\mu|$ versus spanwise wavelength λ for different Reynolds numbers at $\alpha = 30^\circ$. Filled symbols show negative real Floquet multipliers, open symbols correspond to complex-conjugate Floquet multipliers, and half-filled symbols represent positive real Floquet multipliers. (a) $Re \leq 225$; (b) $Re \geq 225$.

modes. In the short wavelength region, $\lambda < 2.0d$, the instability modes consist of two modes with negative real multipliers and one mode with positive real multipliers in between.

Figure 4 shows the results of the Floquet instability analysis for the $\alpha = 30^\circ$ angle of attack case. In these simulations, an instability mode is resolved with negative real multipliers, which occur as the Reynolds number is larger than around 182, shown in Fig. 4(a). A number of quasi-periodic Floquet multipliers appear in higher wavelength regions. However, as the Reynolds number increases, the wake is stabilized in the wavelength region $\lambda \gtrsim 2.0d$, see Fig. 4(b).

B. Mode characteristics

Based on the mode distribution found in Subsection III A, more calculations were performed to capture the precise critical values for the different modes. The neutral curves of unstable wavelengths varying with Reynolds number are plotted in Fig. 5 for the three angles of attack. Also included are the most unstable spanwise wavelengths calculated from the maximum multipliers. These curves show clearly the variation of the spanwise wavelength as Reynolds number increases.

At $\alpha = 20^\circ$, in Fig. 5(a), the most unstable wavelength for the mode with negative real multipliers, in low Reynolds number range, increases with Re. This mode starts at $Re \approx 400$ with $\lambda/d \approx 0.7$ (see Fig. 2(b)), and ends at $Re \approx 505$ with $\lambda/d \approx 0.877$. It forms a closed long and narrow unstable region in the λ/d versus Re map. Another unstable mode with negative real multipliers appears at $Re \approx 540$ with $\lambda/d \approx 0.976$. The most unstable wavelength increases with Re.

At this angle of attack, two quasi-periodic modes are detected at $Re \approx 465$ with $\lambda/d \approx 2.515$, and $Re \approx 553$ with $\lambda/d \approx 0.684$, respectively. The most unstable wavelength for the first one increases with Re, but is nearly constant for the second one. In the three-dimensional calculations by Yang *et al.*,[32] the spanwise wavelengths found at $\alpha = 20^\circ$ were $\lambda/d \approx 0.67$ and $\lambda/d \approx 0.75$ for $Re = 450$ and $Re = 500$, at which organized vortex structures are detected. The former data point collapses with the present results and is therefore scarcely visible in Fig. 5(a). Meneghini *et al.*[26] investigated flow past a stalled airfoil. A subharmonic mode and a quasi-periodic mode were found at $Re \approx 456$ with $\lambda/d \approx 0.57$, and $Re \approx 580$ with $\lambda/d \approx 2.1$, respectively. The present results are consistent with these earlier findings.

At $\alpha = 25^\circ$, in Fig. 5(b), the wake first becomes unstable to a mode with negative real multipliers. This mode starts at $Re \approx 266$ with $\lambda/d \approx 0.826$, see Fig. 3(a), with an almost constant value for the most unstable wavelength. This mode evolves to a mode with positive real multipliers from $Re \approx 310$ as the subharmonic frequency is excited in the base flow. With the increase of Re, this mode finally ends at $Re \approx 330$ with $\lambda/d \approx 0.845$, i.e., only 3% longer than at $Re \approx 266$.

As Re increases further three unstable modes appear in sequence at the wavelength range $0 - 2.0d$. These modes are two modes with negative real multipliers and one mode with positive

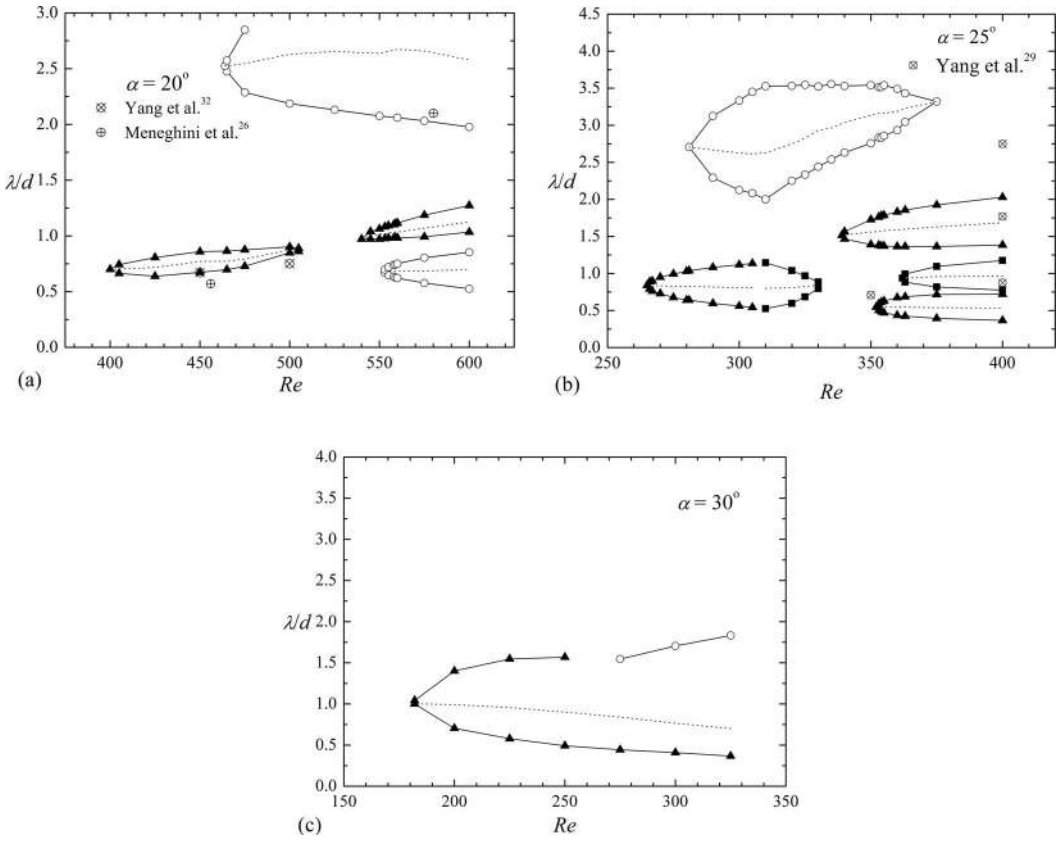

FIG. 5. Neutral stability curves (curves that pass through points where $|\mu| = 1$) and the most unstable wavelengths (curves that pass through points with the maximum $|\mu|$), plotted in a map with Reynolds number (x-axis) and non-dimensional wavelength (y-axis), at angle of attack (a) $\alpha = 20^\circ$, (b) $\alpha = 25^\circ$, and (c) $\alpha = 30^\circ$. Filled triangles represent real and negative multipliers (Mode C), filled squares represent real and positive multipliers (Mode D), and open circles represent complex-conjugate multipliers (quasi-periodic mode). Previous results are also plotted, (a) ⊗, Yang *et al.*;[32] ⊕, Meneghini *et al.*;[26] (b) ⊗, Yang *et al.*[29]

real multipliers. They become critical at $Re \approx 340$ with $\lambda/d \approx 1.519$, $Re \approx 353$ with $\lambda/d \approx 0.545$, and $Re \approx 363$ with $\lambda/d \approx 0.936$, respectively.

The quasi-periodic mode at $\alpha = 25^\circ$ appear at $Re \approx 282$ with $\lambda/d \approx 2.697$. The most unstable wavelength first decreases slightly as Re increases. As the subharmonic frequency is excited in the base flow, the most unstable wavelength starts to increase accompanied with a narrowing of the unstable region. This mode finally ends at $Re \approx 375$ with $\lambda/d \approx 3.321$, see also Fig. 3(b). According to Blackburn and Lopez,[7] two solutions can appear simultaneously in the quasi-periodic bifurcation, corresponding to a traveling wave and a standing wave in the spanwise direction, both modulated by the two-dimensional base flow. However, these aspects are not captured with the Floquet linear analysis, but require a full and nonlinear three-dimensional simulation (Blackburn *et al.*[16]).

For $\alpha = 25^\circ$, Yang *et al.*[29] observed a wavelength of $\lambda/d \approx 0.708$ at $Re = 350$. In their three-dimensional simulations at $Re = 400$, the three dominant wavelengths corresponding to the streamwise vortex structures were $\lambda/d \approx 0.875$, 1.770, and 2.749. The outcome of the linear Floquet analysis is in qualitative agreement with the solution of the full Navier-Stokes equations.

At $\alpha = 30^\circ$, one unstable mode with negative real multipliers is found with the most unstable wavelength decreasing as Re increases, see Fig. 5(c).

A subharmonic mode, which is reported as mode C by Carmo *et al.*[9] and Sheard *et al.*,[11] has a symmetry representation as

$$\text{Mode C}: \ \tilde{\omega}_x(x, y, z, t) = -\tilde{\omega}_x(x, y, z, t + T). \tag{7}$$

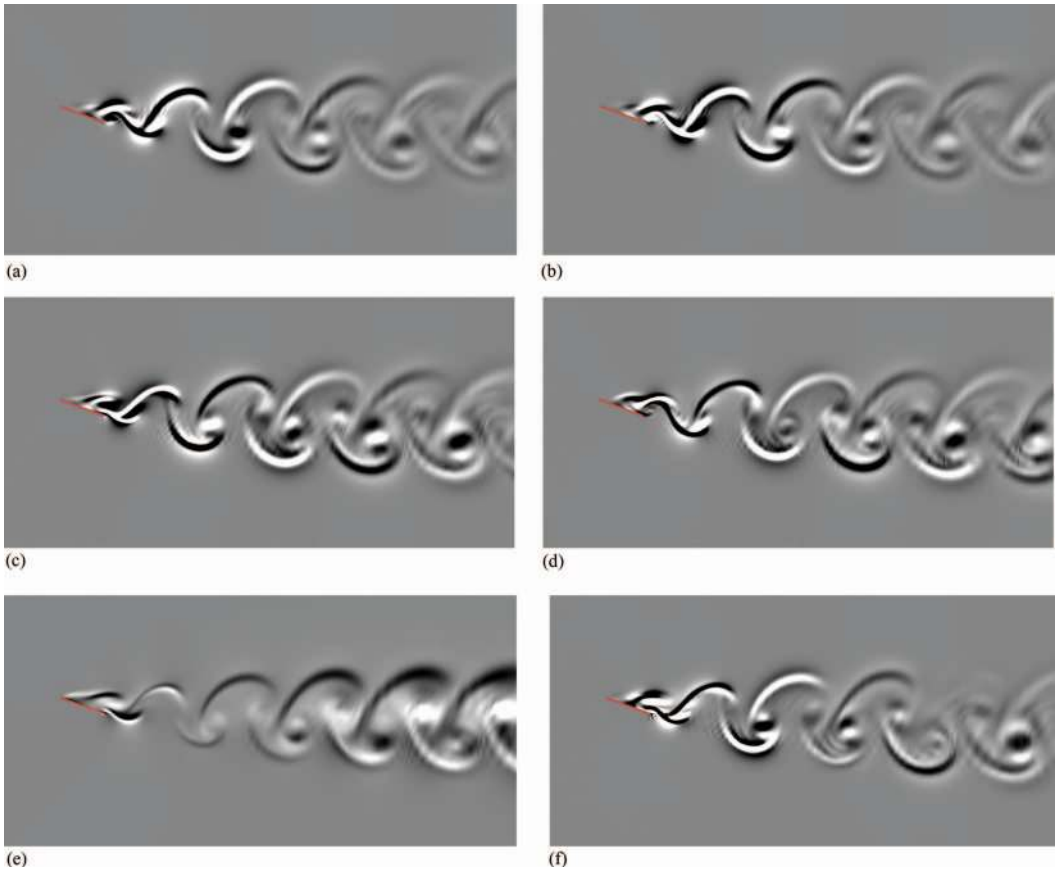

FIG. 6. Plots of streamwise vorticity ω_x for the angle of attack $\alpha = 20^\circ$ case. (a) and (b) Mode C, $Re = 405$, and $\lambda / d = 0.70$, images (a) and (b) are separated by one shedding period, (c) Mode C, $Re = 505$, and $\lambda / d = 0.88$, (d) Mode C, $Re = 540$, and $\lambda / d = 0.98$, (e) Mode QP, $Re = 465$, and $\lambda / d = 2.52$, (f) Mode QP, $Re = 553$, and $\lambda / d = 0.68$.

The inclination of the flat plate with respect to the incoming flow inevitably breaks the symmetry of the wake about the centerline and therefore enables sub-harmonic modes with real and negative multipliers to develop. The wake behind an inclined plate is therefore distinctly different from the symmetric wakes behind circular cylinders and normal flat plates in which only synchronous modes (with real and positive multipliers) and quasi-periodic modes (with multipliers in complex conjugates pairs) develop.

At each of the mode peaks for the three angles of attack in Figs. 2–4, streamwise vorticity plots are exhibited in order to reveal the spatio-temporal symmetry of each instability mode. These vorticity plots are shown in Figs. 6–9.

Figure 6 shows the streamwise vorticity for the instability peaks in Fig. 2. The first peak in Fig. 2(a) is revealed to have topology equal to that of mode C in the wake of a stalled airfoil at $\alpha = 20^\circ$ case, by Meneghini *et al.*,[26] and the wake of a square cylinder which is inclined at angle of attack range $7.5^\circ - 37.5^\circ$, by Sheard *et al.*[11] This mode is subharmonic with period $2T$. Sheard *et al.*[11] has shown that this mode is consistent with the mode C instability discovered in the wake behind rings (Sheard *et al.*[8]), and also observed behind offset tandem cylinders by Carmo *et al.*[9]

Figures 6(a)–6(d) show the subharmonic Floquet mode. The vorticity contours are observed to alternate between Figs. 6(a) and 6(b) over one shedding period. The streamwise vorticity contours for quasi-periodic mode with complex multipliers found at $\alpha = 20^\circ$ are shown in Figs. 6(e) and 6(f).

Figure 7 shows the streamwise vorticity of unstable modes found at $\alpha = 25^\circ$. As with the $\alpha = 20^\circ$ case, the first peak in Fig. 3(a) corresponds to a subharmonic mode, in Fig. 7(a). Due to the vortex interaction, as $Re > 305$, a subharmonic frequency was excited in the base flow. Here, vortex

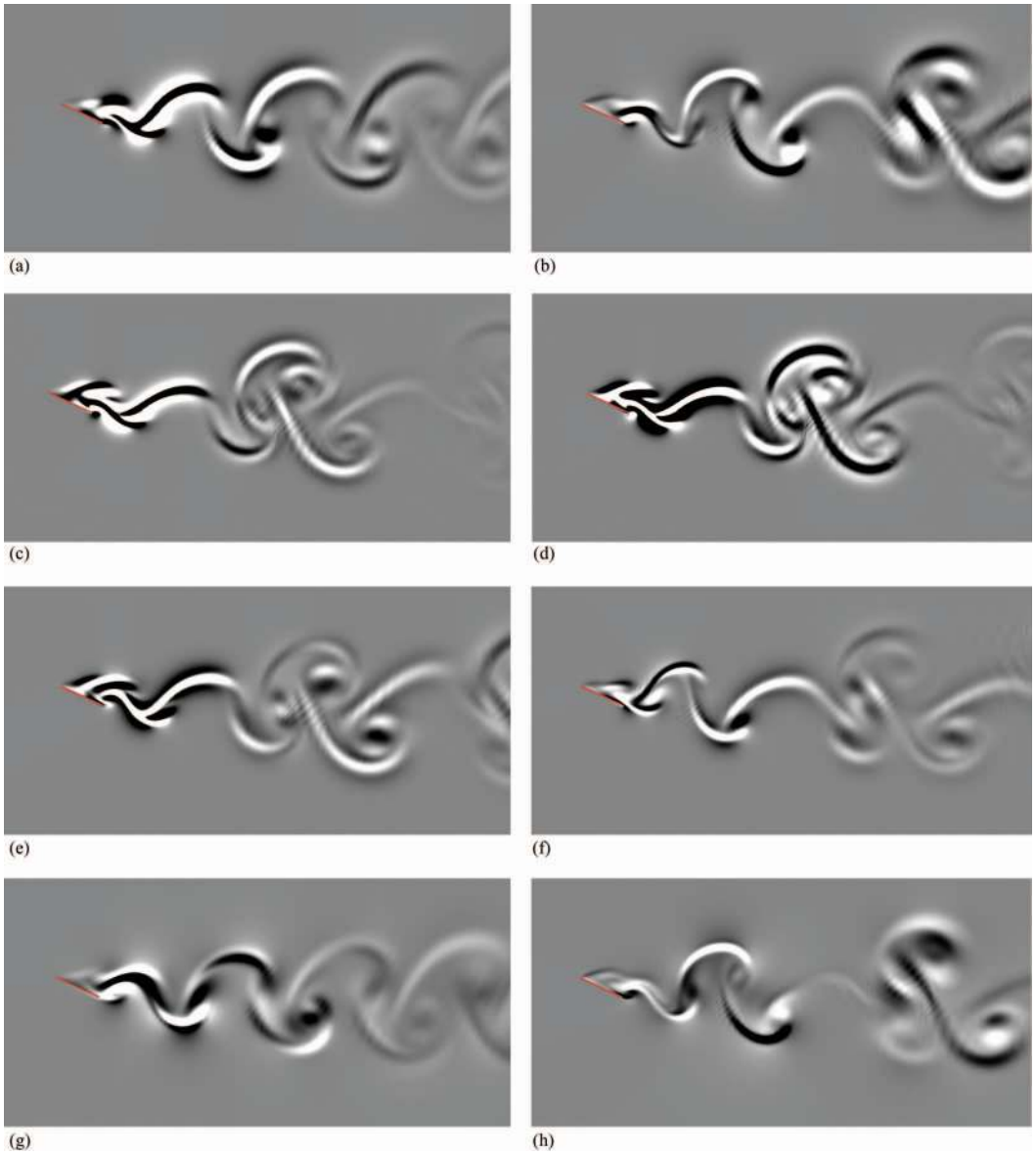

FIG. 7. Plots of streamwise vorticity ω_x for the angle of attack $\alpha = 25^\circ$ case. (a) Mode C, $Re = 266$, and $\lambda/d = 0.83$, (b) Mode C, $Re = 340$, and $\lambda/d = 1.52$, (c) and (d) Mode C, $Re = 353$, and $\lambda/d = 0.55$, image (c) and (d) are separated by two shedding periods, (e) Mode D, $Re = 330$, and $\lambda/d = 0.84$, (f) Mode D, $Re = 363$, and $\lambda/d = 0.94$, (g) Mode QP, $Re = 282$, and $\lambda/d = 2.69697$, (h) Mode QP, $Re = 375$, and $\lambda/d = 3.32$.

interaction refers to the tendency of vortices to pair without affecting the symmetry of the wake, see, e.g., the detailed discussion by Zhang *et al.*[27] The mode C found as $Re \leq 305$ transfers to a new instability mode, called mode D in the present study. This mode possesses positive real multipliers. The vorticity contours for mode D are shown in Figs. 7(e) and 7(f) and the mode is represented by filled squares in Fig. 5(b). The mode possesses positive and real Floquet multipliers and exhibits symmetry properties different from modes A, B, and C. In the present 2D base flow, a subharmonic frequency is excited due to vortex interaction. The same vortex pattern will therefore appear twice during the primary shedding period T and the period of the wake is therefore $2T$.

The evolution of the vorticity contours within $2T$ is shown in Fig. 8 for $Re = 330$ and $\lambda/d = 0.84$. In Fig. 8, we clearly see the vortex interaction from the spanwise vorticity in the base flow which is represented by solid contour lines. The corresponding Floquet mode is

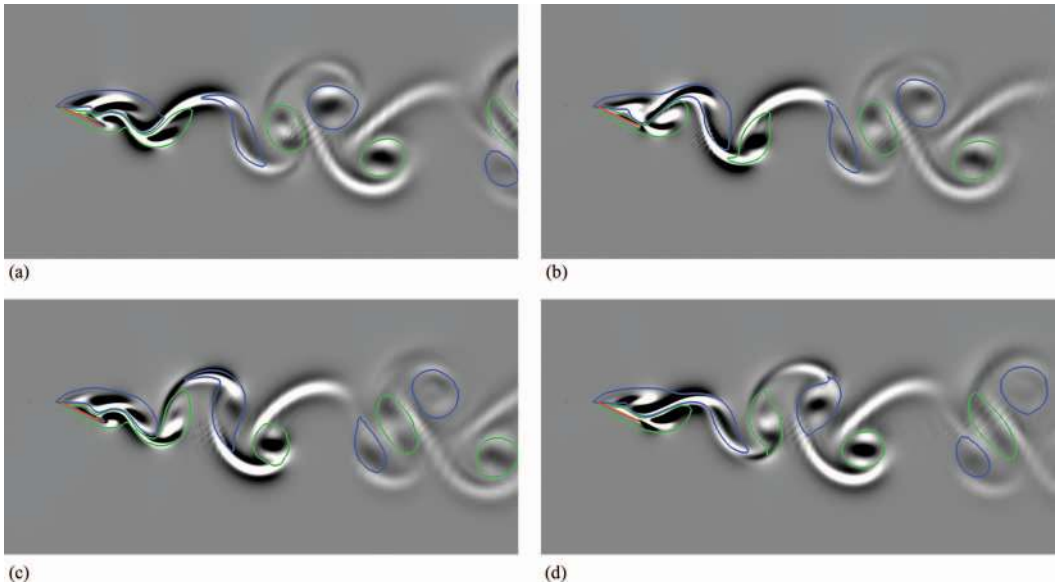

FIG. 8. The near wake topology for mode D, at $\alpha = 25^\circ$, $Re = 330$, and $\lambda / d = 0.84$. Represented are the base flow vorticity in spanwise direction (solid blue and green lines) and the streamwise vorticity for mode D (black and white contours). Images (a)–(d) are separated by half of the shedding period T.

represented by the grayscale background. It is evident that there is no reflectional symmetry or alternate vorticity with opposite sign between the perturbation fields that are one shedding period apart. The spanwise vortices are convected downstream and this process repeats itself every second period.

As Re increases, the peaks in Fig. 3(e) correspond to the modes appearing sequentially. These are two subharmonics modes, see Figs. 7(b)–7(d), and a mode the same as mode D, shown in Fig. 7(f). Figures 7(c) and 7(d) show the alternate vorticity contour separated by $2T$. The contours exhibit the topology of the subharmonic mode with vortex interaction in the base flow. Since the subharmonic frequency is excited in the base flow, the period of the base flow is $2T$. The Floquet mode changes sign every $2T$ and therefore exhibits the same symmetry as mode C.

Figures 7(g) and 7(h) show the vorticity contours for the quasi-periodic mode at $\alpha = 25^\circ$. The difference between the two mode topologies is the existence of vortex interaction in the second one, see Fig. 7(h).

The 2D wake flow past an inclined flat plate was investigated in detail by Zhang *et al.*[27] The results revealed a route of the transition from steady to chaotic flow and summarized the variation of the Strouhal number and the wake pattern. For $\alpha = 25^\circ$, a period-doubling was observed together with various incommensurate bifurcations which coexisted in the flow system. The present study is

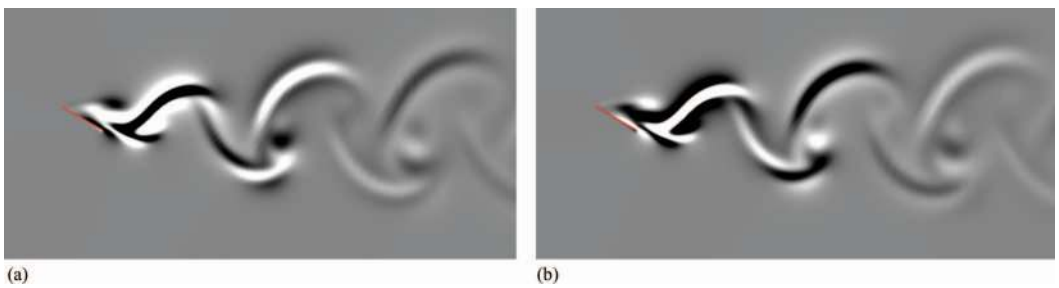

FIG. 9. Plots of streamwise vorticity ω_x for the angle of attack $\alpha = 30^\circ$ case. (a) and (b) Mode C, $Re = 182$, and $\lambda / d = 1.02$. Images (a) and (b) are separated by one shedding period T.

consistent with their findings. In particular, the vortices which develop in the wake have a tendency of pairing over twice the primary shedding period.

Figure 9 shows the streamwise vorticity of the most unstable Floquet mode at angle of attack $\alpha = 30^\circ$. This mode displays the same spatio-temporal symmetry consistent with mode C observed for the other two angles of attack.

IV. CONCLUSIONS AND REMARKS

A Floquet analysis has been performed at three different angles of attack in order to assess in some detail the three-dimensional stability modes of the wake behind an inclined flat plate. Linear Floquet stability analysis is a viable tool to explore when a time-periodic two-dimensional wake behind a bluff body experiences a transition to three-dimensional flow and to identify the spanwise wavelength of the three-dimensional modes. The method is attractive since a wide range of parameter values can be considered, but its applicability is limited to linear growth of the disturbances since nonlinear effects are neglected. In order to capture nonlinear growth, solutions of the full Navier-Stokes equations are required.

The same three angles of attack were considered here as in our accompanying paper (Yang *et al.*[28]) where results from three-dimensional Navier-Stokes calculations were presented. Independent of the angle of attack, however, the time-periodic two-dimensional flow transitions to three-dimensional flow through a sub-harmonic mode C instability, as summarized in Table II. With increasing angle of attack, the transition occurs at a lower critical Reynolds number Re_{cr} but with an increasing spanwise wavelength λ / d. To account for the different angle of inclinations, the effective width of the plate $d' = d\sin\alpha$ felt by the free stream might be a more appropriate length scale than d. The corresponding Reynolds number Re'_{cr} at which the transition to three-dimensional flow occurs still decreases with increasing α. However, the spanwise wavelength turns out to be close to $2.0d'$ for all attack angles. For the particular angle of attack $\alpha = 25^\circ$, Yang *et al.*[29] observed that the spanwise wavelength deduced from their two-point correlation data remained close to $2.0d'$ over a fairly wide range of Reynolds numbers from 300 to 800.

It is noteworthy that this short wavelength mode with negative real Floquet multipliers exists only in the range from $Re = 400$ to $Re = 505$ until it again emerges at $Re = 540$ for $\alpha = 20^\circ$. The wake flow is thus stable with respect to short wavelength instabilities in the Reynolds number interval from 505 to 540. However, a quasi-periodic long wavelength mode develops for Reynolds numbers above 465. A similar bifurcation scenario was observed for $\alpha = 25^\circ$. The first short-wavelength instability can be seen from $Re = 266$ to 330, followed by a narrow gap between 330 and 340 where the wake is stable with respect to short-wave disturbances. However, while the unstable wavelength was increasing with Re for $\alpha = 20^\circ$, the most unstable wavelength remained almost constant for $\alpha = 25^\circ$ even though the unstable mode changes from having negative to positive real Floquet multipliers at $Re \approx 310$. This happened because a sub-harmonic frequency was excited such that the mode C instability turned into a mode D instability. The substantially simplified neutral stability map for $\alpha = 30^\circ$ suggests that several modes have been suppressed at the highest angle of attack considered here.

Although the validity of the present linear analysis is restricted to the early stages of the transition from two-dimensional to three-dimensional flows, the present results demonstrate the sensitivity of the transition scenario on the angle of attack.

TABLE II. Inception of the first instability of the wake behind an inclined plate. $Re' = U_0 d' / \nu$ is the effective Reynolds number based on the projected plate width $d' = d\sin\alpha$.

Attack angle α	Re_{cr}	Re'_{cr}	λ / d	λ / d'
20°	400	137	0.700	2.05
25°	266	112	0.826	1.95
30°	182	91	1.019	2.04

ACKNOWLEDGMENTS

This work has received support from the Research Council of Norway (Program for Supercomputing) through a grant of computing time.

[1] A. Roshko, "On the drag and shedding frequency of two-dimensional bluff bodies," NACA Technical Note 3169, 1954.
[2] C. H. K. Williamson, "The existence of two stages in the transition to three-dimensionality of a cylinder wake," Phys. Fluids **31**, 3165 (1988).
[3] C. H. K. Williamson, "Vortex dynamics in the cylinder wake," Annu. Rev. Fluid. Mech. **28**, 477 (1996).
[4] D. Barkley and R. D. Henderson, "Three-dimensional Floquet stability analysis of the wake of a circular cylinder," J. Fluid Mech. **322**, 215 (1996).
[5] O. Posdziech and R. Grundmann, "Numerical simulation of the flow around an infinitely long circular cylinder in the transition regime," Theor. Comput. Fluid Dyn. **15**, 121 (2001).
[6] J. Robichaux, S. Balachandar, and S. P. Vanka, "Three-dimensional Floquet instability of the wake of square cylinder," Phys. Fluids **11**, 560 (1999).
[7] H. M. Blackburn and J. M. Lopez, "On three-dimensional quasiperiodic Floquet instabilities of two-dimensional bluff body wakes," Phys. Fluids **15**, L57 (2003).
[8] G. J. Sheard, M. C. Thompson, and K. Hourigan, "From spheres to circular cylinders: The stability and flow structures of bluff ring wakes," J. Fluid Mech. **492**, 147 (2003).
[9] B. S. Carmo, S. J. Sherwin, P. W. Bearman, and R. H. J. Willden, "Wake transition in the flow around two circular cylinders in staggered arrangements," J. Fluid Mech. **597**, 1 (2008).
[10] M. J. Fitzgerald, G. J. Sheard, and K. Ryan, "Cylinders with square cross section: Paths to turbulence with various angles of incidence," in *Proceedings of the 16th Australasian Fluid Mechanics Conference*, edited by P. Jacobs, P. McIntyre, M. Cleary, D. Buttsworth, D. Mee, R. Clements, R. Morgan, and C. Lemckert (School of Engineering, The University of Queensland, 2007), p. 1055.
[11] G. J. Sheard, M. J. Fitzgerald, and K. Ryan, "Cylinders with square cross-section: Wake instabilities with incidence angle variation," J. Fluid Mech. **630**, 43 (2009).
[12] G. J. Sheard, "Wake instability features behind a square cylinder: Focus on small incidence angles," J. Fluid Struct. **27**, 734 (2011).
[13] D.-H. Yoon, K.-S. Yang, and C.-B. Choi, "Three-dimensional wake structures and aerodynamic coefficients for flow past an inclined square cylinder," J. Wind Eng. Ind. Aerodyn. **101**, 34 (2012).
[14] H.-Q. Zhang, U. Fey, B. R. Noack, M. König, and H. Eckelmann, "On the transition of the cylinder wake," Phys. Fluids **7**, 779 (1995).
[15] H. M. Blackburn and G. J. Sheard, "On quasiperiodic and subharmonic Floquet wake instabilities," Phys. Fluids **22**, 031701 (2010).
[16] H. M. Blackburn, F. Marques, and J. M. Lopez, "Symmetry breaking of two-dimensional time-periodic wakes," J. Fluid Mech. **522**, 395 (2005).
[17] K. Ryan, M. C. Thompson, and K. Hourigan, "Three-dimensional transition in the wake of bluff elongated cylinders," J. Fluid Mech. **538**, 1 (2005).
[18] N. K.-R. Kevlahan, "Three-dimensional Floquet stability analysis of the wake in cylinder arrays," J. Fluid Mech. **592**, 79 (2007).
[19] B. S. Carmo, J. R. Meneghini, and S. J. Sherwin, "Secondary instabilities in the flow around two circular cylinders in tandem," J. Fluid Mech. **644**, 395 (2010).
[20] R. S. Gioria, P. J. S. Jabardo, B. S. Carmo, and J. R. Meneghini, "Floquet stability analysis of the flow around an oscillating cylinder," J. Fluid Struct. **25**, 676 (2009).
[21] M. Nazarinia, D. Lo Jacono, M. C. Thompson, and J. Sheridan, "The three-dimensional wake of a cylinder undergoing a combination of translational and rotational oscillation in a quiescent fluid," Phys. Fluids **21**, 064101 (2009).
[22] D. Lo Jacono, J. S. Leontini, M. C. Thompson, and J. Sheridan, "Modification of three-dimensional transition in the wake of a rotationally oscillating cylinder," J. Fluid Mech. **643**, 349 (2010).
[23] D. Richter, E. S. G. Shaqfeh, and G. Iaccarino, "Floquet stability analysis of viscoelastic flow over a cylinder," J. Non-Newtonian Fluid Mech. **166**, 554 (2011).
[24] C.-B. Choi, Y.-J. Jang, and K.-S. Yang, "Secondary instability in the near-wake past two tandem square cylinders," Phys. Fluids **24**, 024102 (2012).
[25] M. C. Thompson, K. Hourigan, K. Ryan, and G. J. Sheard, "Wake transition of two-dimensional cylinders and axisymmetric bluff bodies," J. Fluid Struct. **22**, 793 (2006).
[26] J. R. Meneghini, B. S. Carmo, S. P. Tsiloufas, R. S. Gioria, and J. A. P. Aranha, "Wake instability issues: From circular cylinders to stalled airfoils," J. Fluid Struct. **27**, 694 (2011).
[27] J. Zhang, N.-S. Liu, and X.-Y. Lu, "Route to a chaotic state in fluid flow past an inclined flat plate," Phys. Rev. E **79**, 045306 (2009).
[28] D. Yang, B. Pettersen, H. I. Andersson, and V. D. Narasimhamurthy, "Vortex shedding in flow past an inclined flat plate at high incidence," Phys. Fluids **24**, 084103 (2012).
[29] D. Yang, V. D. Narasimhamurthy, B. Pettersen, and H. I. Andersson, "Three-dimensional wake transition behind an inclined flat plate," Phys. Fluids **24**, 094107 (2012).
[30] G. J. Sheard, T. Leweke, M. C. Thompson, and K. Hourigan, "Flow around an impulsively arrested circular cylinder," Phys. Fluids **19**, 083601 (2007).
[31] G. J. Sheard and K. Ryan, "Pressure-driven flow past spheres moving in a circular tube," J. Fluid Mech. **592**, 233 (2007).
[32] D. Yang, B. Pettersen, H. I. Andersson, and V. D. Narasimhamurthy, "On oblique and parallel shedding behind an inclined plate," Phys. Fluids **25**, 054101 (2013).